# Automatic Levee Extraction along Rivers from High Resolution Terrain Models

Wilfried Karel[1], Carolina Damm[1], Martin Wenk[2], Markus Hollaus[1], Norbert Pfeifer[1]

[1] TU Wien, Department of Geodesy and Geoinformation, 1040 Wien, Austria
(Wilfried.Karel, Carolina.Damm, Markus.Hollaus, Norbert.Pfeifer)@tuwien.ac.at
[2] Federal Ministry of Agriculture and Forestry, Climate and Environmental Protection, Regions and Water Management, 1010 Wien, Austria
Martin.Wenk@bmluk.gv.at

**Keywords:** Digital Terrain Model, levee, LiDAR, terrain analysis, profiles

**Abstract**

To plan nature restoration of fluvial corridors on a national level an inventory of existing man-made levees is mandatory. We suggest an automatic method for a river-wise extraction of levees from a high resolution terrain model based on profiles perpendicular to the river axis. This includes a method to cover corridors with non overlapping profiles with a given maximum distance. Levee detection is based on a mathematical formulation of the protective function of levees, i.e. negative elevation differences in outward direction. In an evaluation of 150 km river length distributed over nine different rivers in Austria the method detected 98% of manually extracted levees, and 68% of their length.

## 1. Introduction

The EU (European Union) Nature Restoration Regulation (Coucil of the European Union and European Parliament, 2024) is a key of the EU Biodiversity Strategy, aimed to restore degraded ecosystems. In this course, EU member states report on restoration possibilities and monitor this process. One of the measures to improve (floodplain) ecosystems is to permit flooding, flooding itself being a natural process. In the last decades, however, numerous rivers were given a trapezoid profile for fast water discharge and confined by levees to protect the area behind them, i.e. the floodplain, from the water. In (Poff et al., 1997) the effect of “levees and channelization” on hydrology, i.e. the reduction of over-bank flows, is discussed, as well as the geomorphic and ecological responses to the altered flow regimes. Removing such artificially constructed levees would allow restoration of floodplain habitats. However, levees are often multi-functional constructions, e.g. providing flood protection and transport by rail or road. Furthermore, in many of those protected areas behind levees economic and social activities developed. Thus, different ecologic, social, economic, etc., factors have to be considered, before opening up a levee. For making good decisions, high quality data is necessary. It must be reliable, homogeneous, and accurate.

In (Galloway et al., 2013) the definition of a levee is a “man-made structure, usually an earthen embankment, designed, and constructed in accordance with sound engineering practices to contain, control, or divert the flow of water so as to provide protection from temporary flooding”. In this article we concentrate on such structures along the river and refer to them as levees. Structures perpendicular to the stream flow include especially the dams, and they are not in the focus of this article.

High quality data on levees is often not available. Reasons for data paucity include, that responsibilities are shared between administrative bodies at different levels and fields, that responsibility changed over the years, that technological developments lead to loss of data, that documentation was neither digitized nor collected in a central database, etc. On a global level the lack of adequate data is discussed in (Lehner et al., 2011) for the case of reservoir dams. The question arises, if man-made levees can be extracted from Earth observation data in an efficient way, thus delivering the required geo-data with the necessary quality w.r.t. reliability, homogeneity, and accuracy.

While there is a homogeneous river network for Austria (Wimmer et al., 2021), and there is also a comprehensive data set of dams and cross-sectional buildings, there is no registry of levees along the rivers. Thus the Federal Ministry of Agriculture and Forestry, Climate and Environmental Protection, Regions and Water Management of the Republic of Austria commissioned a study to explore the possibilities to detect levees along Austria’s river network from the high resolution terrain model. The aim is thus to find and locate levees automatically in Earth observation data, specifically in the 1 m LiDAR DTM (Digital Terrain Model, acquired by airborne scanning with a LiDAR (Light Detection and Ranging) device). All levees which prevent a river from overflowing shall be found, including artificial levees but also naturally occurring levees. The precise geometrical location was not considered to be of utmost importance. Together with other socio-economic and ecological data this can build the basis for assessing nature restoration possibilities, see e.g. the GIS (Geographic Information System) analysis in (Hoenke et al., 2014) for the case of river dams.

Starting from the above question, the contribution of this article is to 1) suggest an algorithm for levee detection along rivers and 2) evaluate this methodology by comparison to manually acquired reference data. Our methodological contribution lies in suggesting a method that can also extract very subtle levees using high resolution data and a carefully crafted extraction approach.

## 2. Related Work on the Detection of Dams and Levees in Earth Observation Data

Given the importance of dams and levees in water management, a number of studies have tried to extract them automatically from images and terrain models. In (Lee et al., 2023) a method is suggested to extract levees and their parameters from LiDAR point clouds acquired with a mobile platform (a

car driving along the levees). This approach confirms using terrain shape information as source for levee extraction, although it is focused on modeling levees rather than extracting them in a large dataset.

(Wing et al., 2019) suggest to use DEM (Digital Elevation Model) features for levee extraction. Similarly, in (Sasaki et al., 2023) it is reported that levees were extracted from a 5 m DEM. In (Khanh et al., 2025) 10 m DEMs were used in 5 different countries to extract levees of major rivers. They used a global water mask to exclude permanent water bodies and a 500 m wide buffer from the river mask for limiting the search space. For detecting levees they computed features for each DEM cell, specifically 1) the height difference of a cell to the lowest elevation in a 70 m square window, 2) maximum slope in the 8-neighborhood, 3) the value of the aspect difference of opposing cells (in the 8-neighborhood) which is closest to 180 °, and 4) a signed curvature measure in the cell. Based on multiple thresholds the cells that fit certain conditions are extracted as levee precursors. Using image processing, precursor extraction results are refined. Obviously, height differences are of importance, and this is also featured in the algorithm suggested by us. On the other hand, we suggest a profile-based approach, which is loosely related to the aspect difference. It is noted that these approaches were developed for 5 m to 10 m terrain models. A different approach is suggested in (Pronk et al., 2026), where depressions in a (30 m grid width) terrain model are the starting point for levee detection.

Higher resolution terrain information is often used to extract breaklines along levees (and other terrain features), see (Bähner et al., 2022) and (Mandlburger et al., 2016). Breaklines are locations of a sharp change (discontinuity) of the first derivative of the surface. This would, however, be too restrictive for the extraction of levees, which are targeted here. They may have more rounded shapes.

Recently, a number of studies was published which use deep learning for the extraction of dams. In (Balaniuk et al., 2020) a method to extract mining tailing dams[1] from Sentinel-2 satellite images is presented. Training data was based on official dam locations but had to be corrected to pin-point dam location. As a deep learning approach was followed, a large amount of training data was necessary. Also the background, i.e. the “no dam” class, had to be trained. The method was applied to the whole area of Brazil. In (Jing et al., 2021) a deep learning approach is suggested to extract reservoir dams from a variety of data sets including OSM, global terrain models, global water data layers and others. After the detection a number of constraints was applied to filter the results. In (He et al., 2025) deep learning is used to generate a global data set of river obstructions including dams. They use deep learning on high-resolution satellite imagery and existing inventories. Manual verification is included to guarantee the quality of the provided data set. As also confirmed by these studies, deep learning approaches require a large and sufficiently diverse set of training data. (Xia and Tonooka, 2024) use satellite images, terrain model and slope with 50 cm raster width as input for a U-Net to extract coastal levees, with training data manually sampled. They report an intersection over union of 0.51.

Extensive sources for levee data include the NLD (National Levee Database of the U.S.) (US Army Corps of Engineers, 2026) and global levees in delta areas (Nienhuis et al., 2022). In (Shiraishi et al., 2025) a global dataset containing 100 000 km of levees is described, extracted from LiDAR DTMs with F1 scores between 0.3 and 0.5.

In comparison to the works above, also very subtle levees shall be detected according to the aim formulated in section 1. Thus, a high resolution terrain model with a spacing of 1 m is used. Concerning machine learning (and deep learning) no appropriate levee training data was available, especially for the high resolution that is targeted in this application – in Austria. Thus, a rule-based approach to extract the levees based on their geometric properties is proposed.

## 3. Data and Study Sites

### 3.1 Topographic base data

The digital terrain model (DTM) used in this study is based on the OGD (open government data) DTM of Austria. Data acquisition is by airborne LiDAR, and it is provided as 1 m raster file. The accuracy of this DTM is specified as “generally $\pm 0.5$ m”, but from experience higher precision of elevation differences over short horizontal distances can be expected, e.g. a std.dev. in elevation of 10 cm. Obviously, this will depend on land cover. The current version can be downloaded from the geo-portal of the Federal Office of Surveying and Metrology[2]. In project HORA 3.0 (Blöschl et al., 2022) the 1 m DTM was hydrologically enforced to remove bridges and the river network was adjusted to the DTM as described in (Wimmer et al., 2021). The river network was adjusted to the DTM as it was deemed more accurate and both datasets were used in nationwide flood hazard mapping (Blöschl et al., 2024).

For the presented study, specifically the following Austrian-wide data sets were used:

- DTM: (Bundesamt für Eich- und Vermessungswesen, 2021).
- River axis poly-lines adapted from (Umweltbundesamt GmbH, 2018) version 12 by (Wimmer et al., 2021), and respective bank poly-line pairs.
- HQ-300 polygons from the nation-wide flood hazard mapping (Blöschl et al., 2022), which describe the extent of a flood with an annuality of 300 years for all rivers. Protection measures are typically dimensioned for HQ-100 events, thus the HQ-300 polygon can be expected to include all flood protection levees.
- Fluvial corridors following the guidelines of the European Union’s ECOSTAT working group (European Commission et al., 2024).
- National borders (Bundesamt für Eich- und Vermessungswesen, 2025).

### 3.2 River study sites

Using the countrywide data sets mentioned in the previous section, the levee extraction algorithm was applied to all Austrian rivers with a minimum catchment size of 10 km$^2$. Altogether these are 2735 river lines with a total river length of approx.

[1] Mining tailing dams are earthworks for safe storage of possibly toxic waste of mining activities.

[2] https://www.bev.gv.at/Services/Produkte/Digitales-Gelaendehoehenmodell.html

32,000 km. The manual extraction of levees with the same coverage would have been disproportionately laborious. Thus, the acquisition of reference data focused on selected rivers.

The rivers were determined via three main criteria. These were the size of the river catchment, the degree of human influence on the river (based on own judgment) , and the location of the river within the different landscapes of Austria. To assess various possible levee forms, the selected rivers should cover a wide range of these criteria.

This resulted in the following nine rivers being used as study sites for the generation of reference data: Drau, Lech, Traun, Leitha, Mürz, Kamp, Rußbach, Brixenbach and Wambach. Figure 1 visualizes their locations in Austria. It also provides an overview of the manually digitized levees serving as reference data.

As intended, the selected rivers possess a variety of characteristics. Their catchment sizes range from $\geq 10\,\mathrm{km}^2$ (Wambach) to $\geq 10{,}000\,\mathrm{km}^2$ (Drau). Moreover, the river Lech represents one of the last near-natural Alpine wild rivers (Kogelbauer, 2022). In contrast, rivers such as the Traun and the Leitha possess visible signs of human intervention, with straight levees narrowing their courses. Furthermore, the rivers span various regions of Austria, ranging from the lowlands in the east (e.g. Rußbach) to the Alps in central and western Austria (e.g. Brixenbach). For a more differentiated river selection based on location, the Austrian ‘Fließgewässer-Bioregionen’ were used. These regions divide Austria into 15 landscapes based on factors such as geology, climate and macrozoobenthos (Wimmer et al., 2012). To sum up, Table 1 provides an overview of the characteristics of the nine rivers. Additionally, it lists the length of the manually digitized levees for each river.

## 4. Methods

We hereby present our methods for extracting levees both automatically and manually, and for how to assess the former’s quality of results using the latter’s outcome as reference.

### 4.1 Automatic levee extraction

Our method for automatic levee extraction exclusively operates on geometry. However, the identification of according distinctive and generally applicable properties turns out to be challenging. Primarily in lowlands, levees may be narrow all along, and barely rise above their hinterland. To facilitate cultivation with agricultural machines, their landside slopes may be notably more gentle than what is required for their stability. While the pedestals of mobile walls may be narrow, motorways and multi-track railroads are wide. Together with varying crown heights, this results in a virtually unlimited range of base-to-height ratios. Especially when serving as transport route, a levee’s crown height both above water and above its hinterland may change considerably along its course. Concerning their ground views, levees may exhibit sharp turns, and be intermitted by passageways for pedestrians or vehicles, to be closed only during flood events. Levees that carry transport routes may form junctions, and have access ways. In case of high-speed routes, their shapes may be especially complex. Beyond the needs for flood protection, these are then governed by vehicle dynamics and rain water runoff, with transversely inclined road ways or rail tracks, possibly separated by drainage ditches.

Given their complexity, our method does not fully model levee shapes, but it imposes restrictions on certain properties only. It is mainly built on:

1. the focus on earth works along a river, wherefore profiles perpendicular to the river axis are analyzed, and
2. the levee function, which is to protect its hinterland from flooding. Therefore, levee detection is primarily based on negative height differences when analyzing the profiles outwards.

Based on this, we find outer and inner levee contour lines at half the levee heights. We process each river separately, which allows for assigning each extracted levee to a certain river. For graphical explanations of the method and the values of parameters described below, see Figure 2 and Table 2.

**4.1.1 Areas of interest** The spatial union of HQ-300 polygons, buffered by the distance $b_1$, and ECOSTAT buffers constitutes the countrywide area of interest (AoI). It is thus limited to areas that are permanently flooded, are at risk of being so, or form part of a fluvial corridor. The primary purpose of $b_1$ is to extend the AoI until behind a levee where the according HQ-300 polygon ends just before it. A river’s AoI then follows as the spatial intersection of the polygon formed by its bank line pairs, buffered by the distance $b_2$, and the countrywide AoI. $b_2$ thus defines the maximum half-width of a river’s AoI. To speed up processing and avoid low-quality areas of the DTM abroad, we additionally intersect each river’s AoI with the polygon of national borders, again buffered by $b_2$. For the mentioned data sets, see sec. 3.1. It is noted that for rivers with strong changes of flow direction this buffering can lead to AoIs with inner holes.

**4.1.2 Profiles** A naïve approach to cover the AoI with cross profiles samples base points of constant spacing along the river axis, lays out profiles across, and truncates them to the AoI. While this works well along straight reaches, it exhibits major shortcomings along river bends:

- towards the AoI border, profile density may be excessively high on the insides, while being unacceptably low on the outsides, hampering levee detection;
- profiles may intersect each other, yielding nearby levee detections in profiles of largely different directions. Since our in-profile detection of levees is not fully independent of the profile direction, this would add noise to the course of extracted levees.

We strive to alleviate these flaws with a dedicated layout and truncation of profiles.

**Adaptive inter-profile distances per river side** We define the inter-profile distance of convergent profiles as the one between their base points. For divergent profiles, we add to this distance the length of a circular arc having as radius their maximum length, and as angle the one subtended by their directions. For parallel profiles, these two definitions are equivalent.

Aiming at both a minimal and sufficient sampling of the AoI with profiles that start at the river axis, we separately lay out profiles on each river side. We model the river axis as a cubic spline curve embedded in 2D, and use its inflection points

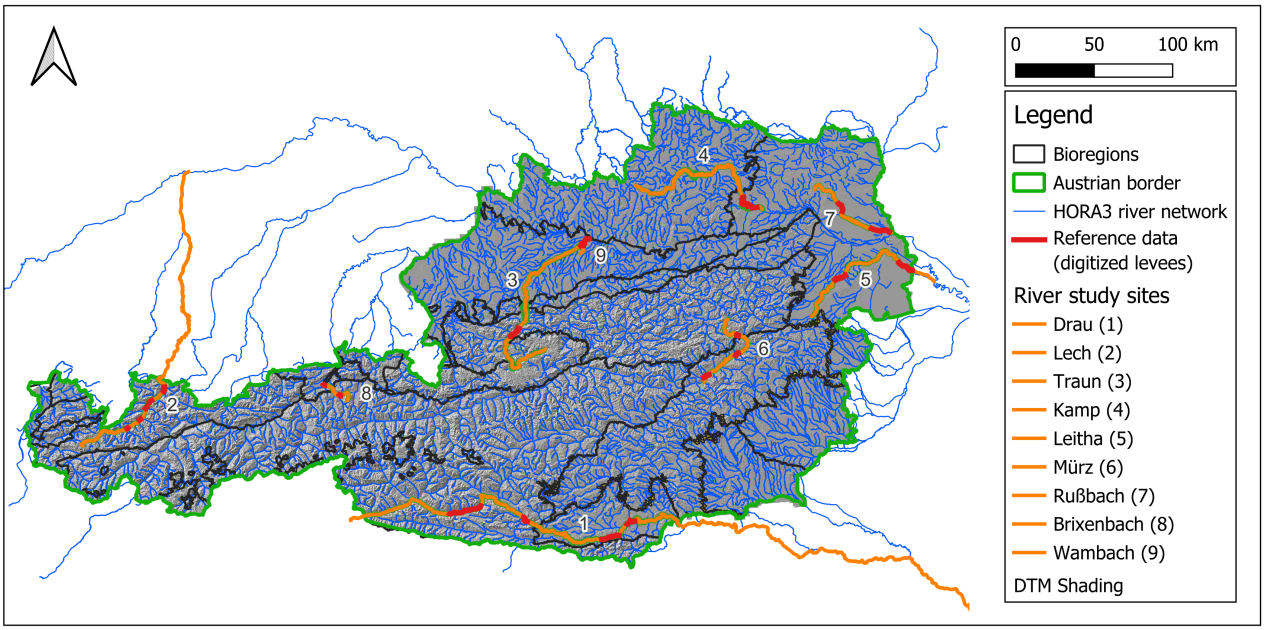


Figure 1. River study sites (orange) and digitized levees acting as reference data (red) on top of the HORA3 river network (blue)

Table 1. Characteristics of the studied rivers, lengths of their inspected reaches, lengths of the manually found levees, and true positive rates of the automatic method. N.B.: ‘Recall’ is the result of applying the suggested method.

| Name | Catch-ment [km$^2$] | Total length [km] | Human influ-ence | Bioregion | Inspected length [km] | Digitized levees [km] | Recall [%] |
|---|---|---|---|---|---|---|---|
| Drau | 10,000 | 676 | medium | Inner Alpine Basin / Southern Alps / Unglaci-ated Central Alps | 55.29 | 56.70 | 70 |
| Lech | 4,000 | 256 | small | Northern Limestone Alps | 16.30 | 12.98 | 46 |
| Traun | 4,000 | 156 | high | Northern Limestone Alps / Limestone Prealps / Bavarian–Austrian Alpine Foreland | 15.15 | 20.50 | 61 |
| Leitha | 1,000 | 121 | high | Eastern Lowlands and Uplands | 19.51 | 41.46 | 69 |
| Mürz | 1,000 | 84 | high | Limestone Prealps / Landscape of Mountain Ridges and Foothills of the Central Alps | 9.55 | 10.03 | 54 |
| Kamp | 1,000 | 169 | medium | Eastern Lowlands and Uplands / Granite and Gneiss Region of the Bohemian Massif | 17.02 | 24.32 | 76 |
| Rußbach | 500 | 74 | high | Eastern Lowlands and Uplands | 18.90 | 38.44 | 76 |
| Brixenbach | 100 | 27 | medium | Limestone Prealps / Unglaciated Central Alps | 2.98 | 3.69 | 60 |
| Wambach | 10 | 8 | high | Bavarian–Austrian Alpine Foreland | 1.87 | 2.64 | 59 |
| Total | | | | | 156.57 | 210.79 | 68 |


https://doi.org/10.5194/isprs-annals-XI-2-2026-897-2026  

as the only base points shared by profiles on either side. In between pairs of subsequent inflection points, neighboring profiles are convergent on one side, and divergent on the other, except in between undulation points, where profiles are parallel. For convergent and parallel profiles, we evenly distribute additional base points along the axis, just enough to undercut a given maximum inter-profile distance. For divergent profiles, we recursively introduce a new profile midway between base points, truncate it to the AoI, and stop the recursion as soon as the given maximum distance is reached.

Our levee detection method only requires profiles to start within, and hence base points to be located somewhere on the river. Hence, the spline used to model the river axis only approximates the poly-line vertices, where the weight of each vertex follows from the reciprocal of the local river width. This reduces the number of inflection points, also by suppressing meanders induced only by noise in the axis poly-line, and it largely ensures that the axis stays between its banks.

**Voronoi truncation** To gain profiles that are free of intersections and that sample the terrain closest to their own base point, we truncate each profile to the segment where its own base point is the closest one. This is efficiently done by computing the Voronoi diagram of all base points, and then intersecting each profile with its base point's Voronoi polygon. As we model the axis with a cubic spline, thus having a minimum total and continuous curvature, this procedure truncates neighboring profiles to similar lengths, and results in profiles that are rather long.

**Thinning** For diverging profiles, the maximum inter-profile distance may be undercut considerably after truncation, as during their layout, their spacing was governed by their former lengths. Hence, to speed up further processing, we now drop as many profiles as possible without violating that maximum distance.

**Discretization in 2.5D** The above results in profiles being directed line segments embedded in 2D that start at the river axis. We now convert them into polylines by sampling vertices along each segment, whose heights we interpolate in the DTM, and where we choose the DTM resolution as their spacing (the intra-profile distance). Due to the same, constant spacing, and because vertices are located along a straight line in 2D, a rigid raster warp can handle the interpolation.

**4.1.3 Detection** Starting from the river axis, we analyze the difference $\Delta Z(d) = \mathrm{mzi}(d) - \mathrm{mzo}(d)$ of two sliding maxima along each profile:

1. the maximum of all heights inwards: $\mathrm{mzi}(d) = \max_{0 \le j \le d} Z_j$;
2. the maximum of heights over some $d_o$ meters outwards: $\mathrm{mzo}(d) = \max_{d \le j \le d+d_o} Z_j$.

The locations where $\Delta Z$ becomes larger than a given detection threshold $\Delta Z_{th}$ we deem as potentially residing on a levee's landside slope. If on a levee, each change of $\mathrm{mzi}$ starts the leg of hinterland that this levee protects. Hence, we reduce the initial list of detection points to the closest ones outwards from each such change. $\mathrm{mzo}$ serves for avoiding detections inside narrow ditches.

With small thresholds $\Delta Z_{th}$ and for levees that carry transversely inclined road ways or rail tracks, the locations found above may not reside on the landside slopes of levees, but on their crowns. In these flat areas, their horizontal progression along a levee may be unsteady. Also, while we consider the landside slope as the most distinctive feature of levee cross-profiles, our primary goal is to map the lines where levees confine the flow of water i.e. lines along their watersides.

To do so, we determine the potential lower ends of landside slopes as the locations where the first derivative of $\Delta Z$ becomes non-negative. For each detection point, we then consider all these lower ends enclosed by its neighboring changes of $\mathrm{mzi}$, using the profile's end if no such change follows. For each pair of a detection point and its potential lower ends in turn, we horizontally intersect the profile midway between $\mathrm{mzi}$ at the detection point, and the height of the putative lower end. Starting from the detection, we use the previous and next such intersections as inner and outer levee contour points for that pair. We choose to intersect at half the levee height, because the slope of levees uses to be the largest there, and so the resulting horizontal positions are well determined. We interpret the horizontal distance between inner and outer contour points as levee width, and reject results that exceed some ample maximum.

The above results in a list of possibly overlapping intervals of inner and outer levee contour points along each profile. From each group of overlapping intervals, we only keep the one with the steepest downward slope of heights, computed between the last change of $\mathrm{mzi}$ before the detection point, and the lower end.

Especially for levees that confine a river just upstream of run-of-river power plants, the water surface may be above their hinterland. In this case, no inner levee contour points may be determined using the above method, or they may reside on fluvial bars, etc., which would again result in unsteady horizontal progressions of their inner contours. Hence, if half the height of a detected levee is hardly above the water surface, we use the intersection of the profile with the according bank line as inner levee contour point.

Most of the above can be applied efficiently to the profiles using discrete, non-linear filters, element-wise Boolean operations, binary search, and a dedicated interval tree to determine overlaps. To increase precision, we linearly interpolate discrete positions. For locating the putative end points, we use forward differences.

**4.1.4 Concatenation and rejection** For each river side, the above results in tuples, where each tuple consists of the inner and outer levee contour points, the point of maximum height in between them, and the originating profile's serial number. We now concatenate points of the same kind, resulting in triples of polylines with common numbers of vertices. While the horizontal positions of points of maximum height are weakly defined on nearly horizontal crowns, our experience shows that the ones of inner contour points tend to be better defined than for the outer ones. Hence, the concatenation of inner contour points results in smoother poly-lines in the horizontal plane, which discriminates them better from lines based on other DTM features. For this reason, the inner ones drive concatenation. To gain poly-lines that are independent of the order in which tuples are processed, we concatenate only points that are mutually nearest neighbors in the horizontal plane, within a given search radius or maximum segment length, respectively. In the search for neighbors, we consider only points from profiles with either a higher or a lower serial number, depending on the search direction. While this procedure concatenates levees

This contribution has been peer-reviewed. The double-blind peer-review was conducted on the basis of the full paper.
https://doi.org/10.5194/isprs-annals-XI-2-2026-897-2026 | © Author(s) 2026. CC BY 4.0 License. 

around corners, it creates only poly-lines with a consistent direction of segments with respect to the flow of water. Finally, we require segments to not cross a third profile, which avoids overlapping polygons formed by pairs of inner and outer contour lines.

We have observed that a levee crown line may be sloped, and while its absolute height may change considerably along its course, that progression is smooth. We thus consider crown height as univariate function of horizontal poly-line length, compare each such function to a smoothed version of it, and drop all poly-line segments where the deviations exceed a certain threshold. This threshold is based on our estimate of the precision of DTM height differences over short distances. Segments dropped from a crown line are also dropped from the corresponding contour lines. To smooth a crown line, we sample points along it with the DTM resolution as horizontal spacing, interpolate their heights in the DTM, and fit a sloped, straight line to these heights for each such point, within a certain symmetric neighborhood. We interpolate DTM heights here to exploit the full DTM resolution also along crown lines i.e. across profiles. To robustly estimate the slope and intercept of locally best-fitting straight lines, we use repeated median regression, with an asymptotic breakdown point of only 50%. Thus, lines that alternately run on crowns and undulated terrain, etc., get truncated close to such transitions.

We finally drop poly-line triples whose inner contour lines undercut a certain minimum length.

For efficient concatenation, we prepare a k-d tree of points in the horizontal plane once for each river side. We iterate over these points, following neighbors to create a poly-line from, and skip these points in subsequent iterations using a hash map.

### 4.2 Reference data extraction

Manual reference data was created by digitizing levees along nine rivers. The rivers themselves are briefly described in section 3.2. The digitization was performed in QGIS using an orthophoto (basemap.at, 2025), a shading of the DTM, and the ‘Elevation Profile’ tool of QGIS. Additionally, the algorithm’s AoIs of the rivers served as guides for the maximum search distances. Apart from that, not all levees along the rivers were digitized but up to four river sections were chosen and their levees extracted. If possible, these sections should stretch evenly along the rivers.

To identify levees for the reference data collection, the definition of (Galloway et al., 2013) mentioned in the introduction was used for orientation. Thus, structures which run roughly parallel to the river, are higher than their surroundings, have a negative slope on the backside, and seem to possess a protective function were digitized as levees. Note that this allows for multiple levees being located behind one another on the same river side. Moreover, he minium crown height for a levee to be identified depended on the amount of terrain undulation nearby. This is in contrast to the levee extraction algorithm, which uses constant height thresholds.

In total, we manually inspected 157 km of the nine rivers, along which we found 211 km of levees. Note that levees can occur on both sides, and multiple levees may also be found on one side of a river.

| Section | Value | Description |
|---|---|---|
| 4.1.1 | 40 m | HQ-300 buffer distance $b_1$ |
| | 300 m | bank polygon and national border buffer distance $b_2$ i.e. max. AoI half-width |
| 4.1.2 | 450 m | max. profile length |
| | 1 m | max. inter-profile distance |
| 4.1.3 | 10 cm | detection threshold $\Delta Z_{th}$ |
| | 9 m | length $d_o$ of the max. height filter outwards |
| | 80 m | max. horizontal distance between corresp. inner and outer contour points |
| 4.1.4 | 3 m | max. concatenated segment length / search radius |
| | 49 m | length of filter for sliding sloped, straight line |
| | 10 cm | max. absolute vertical deviation from this line |
| | 30 m | min. inner contour line length |

Table 2. Parameter values used for automatic levee extraction.

### 4.3 Evaluation

To evaluate automatic levee extraction quality, we combine each pair of inner and outer contour lines into a levee polygon. A levee is considered to be completely detected, if the entire manually extracted crest line is within one of these polygons. A crest line outside of polygons constitutes a false negative. Reasons for such a missing extraction can be errors in the DTM or caused by the algorithm. The DTM is the only source of information for the automatic extraction and mismatches may be caused by random or systematic errors in the DTM, DTM definition (e.g. a building is part of the levee but filtered out in the DTM generation), or temporal decorrelation of DTM and orthophoto. On the other hand, the algorithm simplifies the complex and functional levee definition into a set of geometric rules, and this may also cause missing extractions. The quantitative measures of true positive and false negative are thus augmented by qualitative observations, to understand the cause of errors. False positive detections are considered to be of lesser importance unless they have considerable length (beyond 100 m). They will, therefore, be assessed only qualitatively.

## 5. Results and Discussion

Levees were extracted automatically for the rivers described in sec. 3.2 using the parameters listed in Table 2. See Figure. 2 for results along the Kamp river together with the reference data.

With the terrain model as base data for levee extraction, it is obvious that only permanent levees can be extracted. Mobile flood protection can therefore not be extracted. Although its base is in some cases permanent, this is, by definition, not contained in the digital terrain model. Also closed rows of houses acting as flood protection are not extracted. While houses are obviously sufficiently large to be captured by airborne laser scanning and representation in a 1 m-raster, narrow walls acting as flood protection are not represented in the terrain model and even their representation in the original point cloud may not be sufficient for their extraction.

From all levees extracted manually, 98% were detected at least partially with the suggested algorithm. In Table 1, last column,

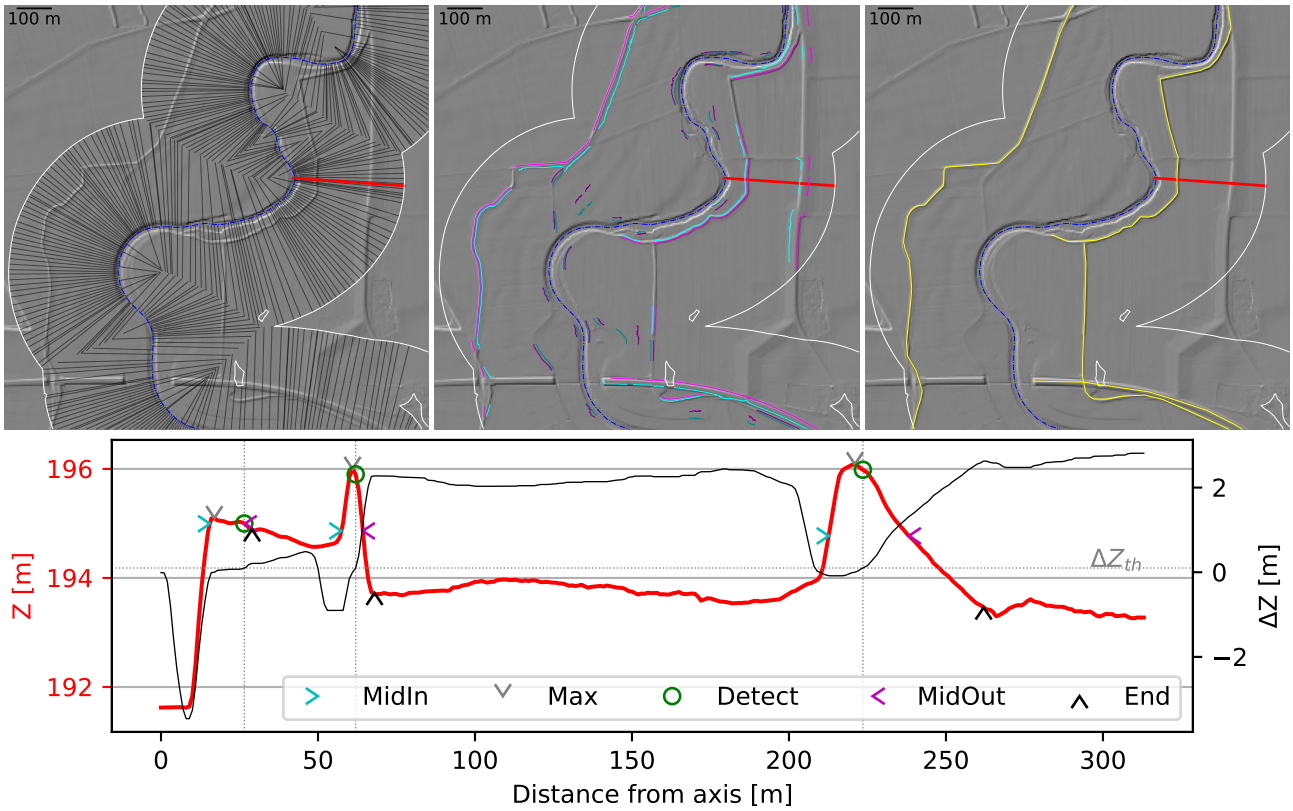


Figure 2. Part of the manually inspected Kamp river reach. Top row: DTM shading overlaid with the river axis (blue), the AoI (white), and an example profile (red). Left: profiles laid across the axis (black), showing only every 25$^{th}$ for readability. Center: inner (cyan) and outer (magenta) levee contour lines automatically extracted from these profiles. Levees with a maximum height below 40 cm are shown in darker shades. Right: manually extracted levee center lines (yellow). Bottom: elevation view of the example profile (red), showing three groups of points: initial detections (Detect), at maximum height (Max), at the lower ends of levee outwards slopes (End), and contour points at mid height on both sides (MidIn, MidOut). The innermost group is dropped in a later step, and so is absent from the central plot of the top row. The detection threshold $\Delta Z_{th}$ gets applied to the sliding difference $\Delta Z$ shown in black.

the proportion of true positive detections is given in percent of levee length. This ranges from 46% at the near natural river Lech to 76% for the rivers Kamp and Rußbach, which differ in morphology and human impact. The average w.r.t. levee length is 68%, whereas the macro average is 63%.

A closer inspection gives insight into discrepancies between reference and automatic levee detection. False negatives in the order of a few meter occur typically at the end of true positive detections. The reference sometimes also continues along a street which is over long stretches a levee but runs without elevation above the surrounding terrain in other areas. In the reference also two parallel levees can be given on one river side, with the outer levee below the elevation of the inner levee. Such an earth work has no protective function when analysis is restricted to the profile (as done in the approach presented here). Finally, at a number of places the reference runs slightly outside the detected levee outline at middle height. Summarizing, the automatic detection and the manual reference feature (slightly) different realizations of a levee definition.

There is also a number of cases, where assumptions within the profile-based algorithm prevent the detection. At elevated street crossings the detection is discontinued. The street running along the river is correctly detected, but the second street runs across the river, preventing the continuation. Short terrain features, which are similar to a (short) levee but at higher level than a (long) levee further outside, cause missing, typically discontinued, detection of the relevant levee. Finally, missing detection can occur in complex topographic situations (oxbow river morphology) where the Voronoi-based profile truncation gives preference to profiles running eventually along a levee. This can happen at sharp river turns and is also found in Figure 2 (lower part) at the half circle the river describes.

Some missing detections occur because the profiles do not reach the boundary of the AoI. This can happen at reservoirs, where the river width is much larger than in free flowing river reaches. In similar situations, where the normal water level is higher then the surrounding terrain, the detected inner points are shifted to the bank line. With a terrain model describing a (wrongly) uneven water surface, this can cause wide horizontal shifts between those bank line points. Therefore, consecutive detections do not get concatenated. In such cases the outer contour line at medium height is often the smoother one. Finally, a detection is only processed further, if a point with non-negative slope is found further outside its profile. In some cases the profile is not sufficiently long enough.

False positive detections can occur at small round mounds. They are typically short. Longer false positive detection are found along street ramps running up to a correctly found levee. The difficulty of automatic methods to correctly identify levees with a small number of commission and omission errors is also found in the articles referenced in Section 2, see (Jing et al., 2021, Xia and Tonooka, 2024, He et al., 2025), necessitating,

This contribution has been peer-reviewed. The double-blind peer-review was conducted on the basis of the full paper.
https://doi.org/10.5194/isprs-annals-XI-2-2026-897-2026 | © Author(s) 2026. CC BY 4.0 License.

e.g., post-processing. While specific objectives and accuracy metrics are too heterogeneous for comparison, there is obviously ample room for improvements with all those methods. However, in this respect it may be worthwhile to follow a research path of global levee data harvesting and homogenization as input for deep learning on high resolution terrain models.

The manual extraction was used as error-free reference. Some advantages of manual compared to automatic levee extraction are that a human digitizer is able to identify long stretches of continuous levees because she small irregularities and gaps are ignored. Further reasons are the ability to consider abrupt changes in direction and to continue a levee beyond the border of the algorithm's AOI. Second, humans can assess the protective function of a levee by looking for man-made structures behind it and by comparing the levee to the elevations of its surroundings. To sum up, setting the levee into context with its environment (in a structural and functional way) is a skill a human digitizer is more equipped for than the algorithm.

Of course, manual levee extraction also has its disadvantages. The first one is speed. It takes much longer to digitize manually than automatically. In our reference data acquisition, a lower boundary for digitization speed is around 15 km river reach per hour, but with large dependence on river morphology and topographic situation. A second strength of the algorithm is its consistency. As humans get tired, they can make mistakes, and naturally generate output based on subjective perception. Concerning perception, some general difficulties in identifying levees were encountered. While it was easy to detect them in flat terrain (e.g., Leitha, Rußbach), it became more difficult in mountainous areas (e.g., Lech, Traun). In these regions levees seemed relatively short and split up, being located in valleys between mountain ranges. Another difficulty arose when identifying levees within populated areas, for example within cities or villages. This was often due to a variety of structures inside the DTM. These structures might stem from the incomplete removal of buildings or might simply reflect greater terrain diversity. One last major factor impacting the levee identification was the river size. Naturally, the larger the river, the easier it was to identify correspondingly large levees.

## 6. Conclusions

A method to detect levees in a high resolution (1 m grid spacing) digital terrain model along given river axes was presented. It operates on profiles, extracts points on half the levee height on the inner and outer slope as well as the levee crown, and eventually concatenates these points to crown lines and levee polygons, respectively. The comparison to manually extracted levee crown lines shows 1) the effectiveness of the method (98% of all levees are detected at least partly), 2) improvement paths within the profile based levee detection and their concatenation, 3) the generalization of the manually acquired reference data, and 4) limitation of the DTM in complete levee representation, caused, e.g., by the ground/off-terrain classification during DTM generation from laser scanning point clouds.

**Acknowledgments** This study is financed by the Federal Ministry for Agriculture and Forestry, Climate and Environmental Protection, Regions and Water Management, Republic of Austria, who provided all the data used.

**Data and code availability** The DTM and Austria's national borders are OGD and can be downloaded from the open government data site of Austria and from the GEO portal of the Federal Office of Surveying and Metrology, respectively. In addition to code, the non-OGD input data of river axes and bank lines, HQ-300 polygons, and fluvial corridors are available via the Git repository (Karel et al., 2025). This also includes reference data as described in section 4.2

## References

Bähner, M., Fuchs, Y., Schäfer, S., 2022. Cannys edge detector: A versatile image processing method applied in hydraulic engineering. *Proceedings of the 39th IAHR World Congress*, International Association for Hydro-Environment Engineering and Research (IAHR), Spain, 4931–4940.

Balaniuk, R., Isupova, O., Reece, S., 2020. Mining and tailings dam detection in satellite imagery using deep learning. *Sensors*, 20(23), 6936.

basemap.at, 2025. Orthofoto. `https://stp.wien.gv.at/basemap`. Last accessed October 2025.

Blöschl et al., 2022. HOchwasserRisikozonierung Austria 3.0 (HORA 3.0). *Österr. Wasser-Abfallwirtsch.*, 74(5-6).

Blöschl, G., Buttinger-Kreuzhuber, A., Cornel, D., Eisl, J., Hofer, M., Hollaus, M., Horváth, Z., Komma, J., Konev, A., Parajka, J., Pfeifer, N., Reithofer, A., Salinas, J., Valent, P., Výleta, R., Waser, J., Wimmer, M. H., Stiefelmeyer, H., 2024. Hyper-resolution flood hazard mapping at the national scale. *Nat. Hazards Earth Syst. Sci.*, 24(6), 2071–2091.

Bundesamt für Eich- und Vermessungswesen, 2021. Serie ALS DTM Höhenraster 1m Stichtag 15.09.2021. `https://doi.org/10.48677/63fd20c5-cd34-4d00-829f-a1fd380f6b4b`.

Bundesamt für Eich- und Vermessungswesen, 2025. Verwaltungsgrenzen (VGD) INSPIRE Stichtag 01.04.2025. `https://doi.org/10.48677/bf810ec9-3869-4290-96d2-cc1d2d5196e5`.

Coucil of the European Union, European Parliament, 2024. Regulation (eu) 2024/1991 of the european parliament and of the council of 24 june 2024 on nature restoration. `http://data.europa.eu/eli/reg/2024/1991/oj`.

European Commission, Joint Research Centre, van de Bund, W., Bartkova, T., Belka, K., Bussettini, M., Calleja, B., Christiansen, T., Goltara, A., Magdaleno, G., Mühlmann, H., Ofenböck, G., Parasiewicz, P., Peruzzi, C., Schmitt, K., Schultze, A., Reckendorfer, W., Bastino, V., 2024. *Criteria for identifying free-flowing river stretches for the EU Biodiversity Strategy for 2030*. Publications Office of the European Union, Luxembourg. `https://data.europa.eu/doi/10.2760/402517`.

Galloway, G., Committee on Levees and the National Flood Insurance Program Improving Policies and Practices, Water Science and Technology Board, Division on Earth and Life Studies, National Research Council, 2013. *Levees and the national flood insurance program*. National Academies Press, Washington, D.C., DC. `https://doi.org/10.17226/18309`.

He, M., Niu, J., Riley, W. J., Shen, C., Zheng, Y., Melack, J. M., Gui, D., Qiu, H., Xie, M., Sun, L., Liu, D., Fu, Y., Wu, Q., Zhou, S., Wu, P., Hu, B. X., 2025. Deep Learning and remote-sensed observations reveal global underestimation of river obstructions. *Water Resour. Res.*, 61(9).

Hoenke, K. M., Kumar, M., Batt, L., 2014. A GIS based approach for prioritizing dams for potential removal. *Ecol. Eng.*, 64, 27–36.

Jing, M., Cheng, L., Ji, C., Mao, J., Li, N., Duan, Z., Li, Z., Li, M., 2021. Detecting unknown dams from high-resolution remote sensing images: A deep learning and spatial analysis approach. *Int. J. Appl. Earth Obs. Geoinf.*, 104(102576), 102576.

Karel, W., Damm, C., Hollaus, M., Pfeifer, N., 2025. Code repository for the automatic levee extraction along rivers from high resolution terrain models. `https://git.geo.tuwien.ac.at/public_projects/levees/-/tree/Toronto`.

Khanh, D. N., Tsumura, Y., Sasaki, O., Shiraishi, K., Akimoto, D., Yamazaki, D., Zhao, G., Hirabayashi, Y., 2025. Mapping the world’s river levees: A hyper-resolution levee database based on digital elevation models. *Geophys. Res. Lett.*, 52(11).

Kogelbauer, B., 2022. DYNAMIC RIVER SYSTEM LECH - Final Report. Technical report, Wasserwirtschaftsamt Kempten.

Lee, J., Yoo, S., Kim, C., Sohn, H.-G., 2023. Automatic levee surface extraction from mobile LiDAR data using directional equalization and projection clustering. *Int. J. Appl. Earth Obs. Geoinf.*, 116(103143), 103143.

Lehner, B., Liermann, C. R., Revenga, C., Vörösmarty, C., Fekete, B., Crouzet, P., Döll, P., Endejan, M., Frenken, K., Magome, J., Nilsson, C., Robertson, J. C., Rödel, R., Sindorf, N., Wisser, D., 2011. High-resolution mapping of the world’s reservoirs and dams for sustainable river-flow management. *Front. Ecol. Environ.*, 9(9), 494–502.

Mandlburger, G., Otepka, J., Briese, C., Mücke, W., Summer, G., Pfeifer, N., Baltrusch, S., Dorn, C., Brockmann, H., 2016. Automatische Ableitung von Strukturlinien aus 3D-Punktwolken. T. Kersten (ed.), *Dreiländertagung der SGPF, DGPF und OVG: Lösungen für eine Welt im Wandel, Publikationen der Deutschen Gesellschaft für Photogrammetrie, Fernerkundung und Geoinformation e.V., Band 25*, 131–142.

Nienhuis, J. H., Cox, J. R., O’Dell, J., Edmonds, D. A., Scussolini, P., 2022. A global open-source database of flood-protection levees on river deltas (openDELvE). *Natural Hazards and Earth System Sciences*, 22(12), 4087–4101. https://nhess.copernicus.org/articles/22/4087/2022/.

Poff, N., Allan, J., Bain, M., Karr, J., Prestegaard, K., Richter, B., Sparks, R., Stromberg, J., 1997. The natural flow regime: A paradigm for river conservation and restoration. *Bioscience*, 47(11), 769–784.

Pronk, M., Gawehn, M., Eleveld, M., Ledoux, H., 2026. Automated levee detection in digital elevation models. EarthArXiv https://doi.org/10.31223/X57X8X.

Sasaki, O., Tsumura, Y., Yamada, M., Hirabayashi, Y., 2023. Automatic levee detection using a high-resolution DEM - Case study in Kinu river basin, Japan. *Hydrol. Res. Lett.*, 17(1), 9–14.

Shiraishi, K., Do, K. N., Sasaki, O., Zhao, G., Yamazaki, D., Boulange, J., Hirabayashi, Y., 2025. Automatic levee detection from lidar dem and its application to global river flood modeling. 38, 341.

Umweltbundesamt GmbH, 2018. Federal reporting water network - flowing water (routes). `http://data.europa.eu/88u/dataset/4a82bfde-26dc-48fc-a706-ee89d3ef70d8`.

US Army Corps of Engineers, 2026. National levee database (NLD). https://levees.sec.usace.army.mil/.

Wimmer, M. H., Hollaus, M., Blöschl, G., Buttinger-Kreuzhuber, A., Komma, J., Waser, J., Pfeifer, N., 2021. Processing of nationwide topographic data for ensuring consistent river network representation. *J. Hydrol. X*, 13(100106), 100106.

Wimmer, R., Wintersberger, H., Parthl, G. A., 2012. Hydromorphologische Leitbilder - Fließgewässertypisierung in Österreich - Band 1: Einführung, Definitionen und Parameter. Technical report, ”Bundesministerium für Land- und Forstwirtschaft, Umwelt und Wasserwirtschaft”.

Wing, O. E. J., Bates, P. D., Neal, J. C., Sampson, C. C., Smith, A. M., Quinn, N., Shustikova, I., Domeneghetti, A., Gilles, D. W., Goska, R., Krajewski, W. F., 2019. A new automated method for improved flood defense representation in large-scale hydraulic models. *Water Resour. Res.*, 55(12), 11007–11034.

Xia, H., Tonooka, H., 2024. Extraction of Coastal Levees Using U-Net Model with Visible and Topographic Images Observed by High-Resolution Satellite Sensors. *Sensors*, 24(5). https://www.mdpi.com/1424-8220/24/5/1444.